Direct Observation of HPL and DG Structure in PS-*b*-PI Thin Film by Transmission Electron Microscopy

Hae-Woong Park, Kyuhyun Im, Bonghoon Chung, Moonhor Ree, and Taihyun Chang*

Department of Chemistry and Polymer Research Institute, Pohang University of Science and Technology, Pohang 790-784, Korea

Koji Sawa and Hiroshi Jinnai*

Department of Macromolecular Science and Engineering, Graduate School of Science and Engineering, Kyoto Institute of Technology, Kyoto 606-8585, Japan

Received December 10, 2006

Revised Manuscript Received February 8, 2007

Introduction

The order−order phase transitions of diblock copolymers often show an epitaxial relationship between the geometries of two phases.[1−11] For example, the transition from hexagonally packed cylinder phase to the body-centered cubic (BCC) phase occurs through initial undulation of the cylinders before they divide into spheres, which eventually converts the cylinder axis to the [111] direction of BCC structure.[4−6,12] The phase transition is known to be reversible, and the reverse transition also follows the same epitaxial course. The transition between the hexagonally perforated lamellar (HPL) to double-gyroid (DG) structure has been also studied extensively.[1,2,13,14] The phase transition is not reversible due to the metastable nature of the HPL phase.[15] Nonetheless, it has been well-established that an epitaxial relationship between the HPL layers and {121} plane of DG structure exists.[1,13,14]

In most studies concerning the epitaxial phase transition from the HPL to DG phase, shear aligned HPL phases were used.[1,14,16] However, the phase transition of the shear aligned HPL layers to DG {121} planes did not maintain their orientation but rotated randomly around the DG [111] axis. In our previous work using the polystyrene-*block*-polyisoprene (PS-*b*-PI) thin film on Si wafer, we observed the epitaxial phase transition from HPL layer to DG {121} plane by grazing incidence small-angle X-ray scattering (GISAXS).[17] In the thin film, the layers in the HPL structure were converted to {121} planes of DG structure maintaining their orientation parallel to the substrate surface. Also, the HPL structure in the thin film exhibits the ABC stacking of the perforations without observable defects. However, we were not able to confirm the block copolymer morphology in the thin films visually by transmission electron microscopy (TEM) due to the difficulty in the sample preparation. In addition, since TEM provides only two-dimensional projections of three-dimensional (3D) entities, obtained TEM micrographs sometimes are not conclusive. One of the solutions for the latter is to use transmission electron microtomography (TEMT).[18] In this Note, we would like to report on the *direct* observations of the HPL and DG structures of PS-*b*-PI thin film as well as the coexistence of the two phases during the phase transition by TEM and TEMT.

* Corresponding authors. T.C.: Tel +82-54-279-2109, Fax +82-54-279-3399, e-mail tc@postech.ac.kr. H.J.: Tel +81-75-724-7846, Fax +81-75-724-7800, e-mail hjinnai@kit.ac.jp.

Experimental Section

Materials. PS-*b*-PI diblock copolymers were synthesized by sequential anionic polymerization. Details of the apparatus and the polymerization procedure were reported previously.[19,20] The PS-*b*-PI was characterized by SEC and ^{1}H NMR (Bruker, DPX-300) to have $M_n = 37\,000$, $M_w/M_n = 1.01$, and the PS content of 38.5 wt %.

TEM. The PS-*b*-PI diblock copolymer solution (10 wt % in toluene) was spin-coated on freshly cleaved mica. The polymer film was vacuum-dried at room temperature for 4 h to remove the residual solvent before annealing in vacuo. The annealed film on a mica substrate was floated on deionized water. The floated film was picked up with a piece of PS thin plate and stained with OsO_4 (Polysciences, 0.4% in water) for 2 h. Then it was embedded in epoxy resin after carbon coating, and the sample was microtomed (RMC Ultracut) normal to the film plane to a nominal thickness of 50−100 nm. The sectioned sample was transferred to a carbon-coated Cu grid (300 mesh) and stained again with OsO_4 for 20 min before taking bright-field TEM (Hitachi-7600) micrographs.

TEMT. TEMT experiments were performed using an energy-filtering transmission electron microscope with a field-emission gun operated at 200 kV (JEM-2200FS, JEOL Co., Ltd., Japan). Projections were collected with a slow-scan CCD camera (Gatan USC1000, Gatan, Inc.). Only the transmitted and elastically scattered electrons (electron energy loss of 0 ± 15 eV) were selected by an in-column energy filter installed in the JEM-2200FS (Omega filter, JEOL, Ltd., Japan) in order to obtain achromatic projections. A series of TEM micrographs were acquired at tilt angles ranging from −60° to +60° at the angular interval of 1°. Subsequently, the tilt series of the TEM micrographs (121 projections) were aligned using with gold nanoparticles as the fiducial markers[21] and then reconstructed on the basis of the filtered-back-projection (FBP) method.[22] All reconstruction procedures were carried out using software developed in our laboratory.

Results and Discussion

The prepared PS-*b*-PI has a composition to shows thermal phase transition from HPL to DG.[17,23] The GISAXS patterns of the PS-*b*-PI thin film show well-developed HPL and DG phases similar to the previous report.[17,24] For the TEM measurements, freshly cleaved mica was used as a substrate to make thin PS-*b*-PI films instead of Si wafer used in the GISAXS study. Mica is a well-known substrate of which the surface property is similar to Si wafer enough for diblock copolymers to exhibit the same wetting behavior,[25,26] i.e., PI block domains are located at both air and substrate interfaces. Unlike Si wafer, mica substrate allows the PS-*b*-PI films to be easily detached by flotation in water.

Figure 1a shows a cross-sectional TEM image of the HPL structure. The sample was annealed at 120 °C for 1 day in vacuo. PI domains were selectively stained by OsO_4 and appear darker than PS domains. Because PS is a minor component of this diblock copolymer, the layers of PS block are perforated by PI blocks. The HPL layers are well aligned parallel to the substrate as expected from the GISAXS pattern.[17] The inset of Figure 1a shows a plan-view of a thinner PS-*b*-PI film (∼350 nm thick) prepared from a more dilute (5 wt % in toluene) solution. Well-ordered and hexagonally perforated structure is observed similar to the AFM images reported by Ludwigs et al.[27,28] To observe the DG phase, the diblock copolymer thin film was annealed at

10.1021/ma062826c CCC: $37.00
Published on Web 03/07/2007

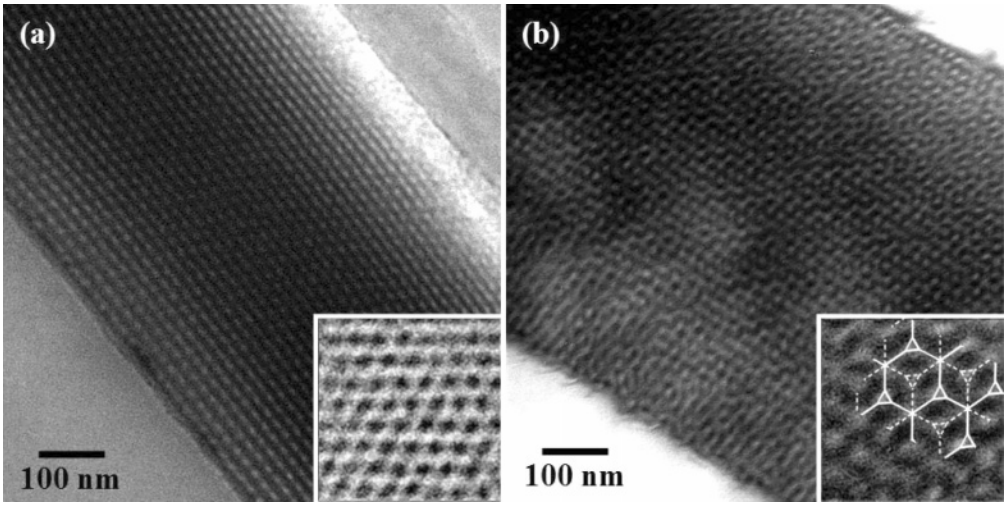

Figure 1. (a) Cross-sectional TEM image of the HPL structure of PS-*b*-PI thin film (~700 nm thick) annealed at 120 °C for 1 day. The inset is a plan-view TEM image (200 nm × 200 nm) of a thinner film (~350 nm thick). (b) Cross-sectional TEM images of PS-*b*-PI thin film annealed at 160 °C for 1 day. Fully developed DG morphology is shown. The complex structure corresponds to DG {111} plane, as shown in the inset of an enlarged TEM image.

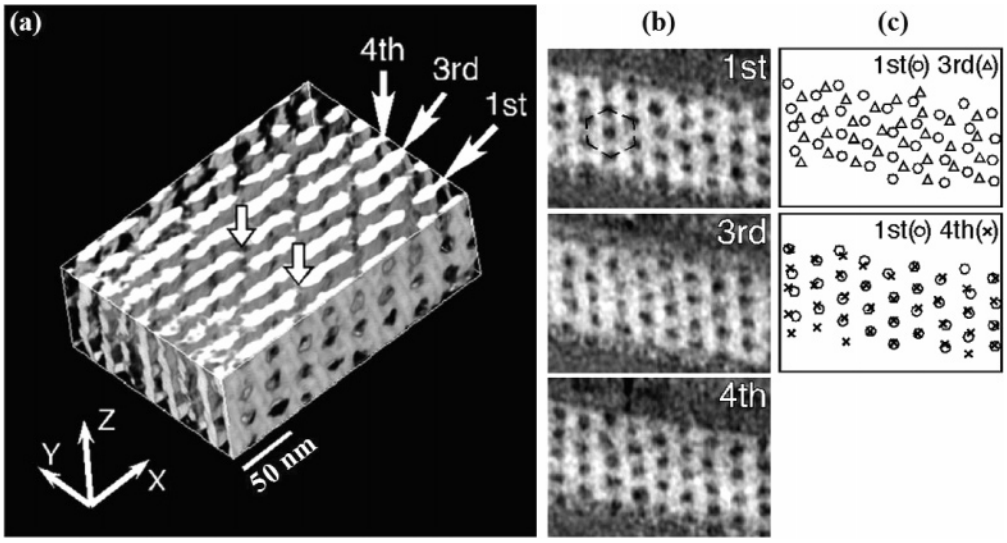

Figure 2. (a) 3D image of the HPL structure obtained by TEMT (260 nm × 180 nm × 90 nm). Only the PS domain is shown for visual clarity. The vertical arrows indicate the position of the perforations. (b) Digitally sliced *x*−*z* planes corresponding to the first, third, and fourth layers showing the position of the perforations. (c) Overlay of the perforation positions: (top) first and third layers; (bottom) first and fourth layers. The ABC type stacking of the perforation is evident from the matching of the first and fourth layers.

160 °C for 1 day. The morphology was fully converted to a well-aligned network structure as shown in Figure 1b, which corresponds to the {111} projection of the DG phase. The {111} plane is perpendicular to the {121} plane, indicating that the DG {121} planes are oriented parallel to the substrate.

Although the layer structure and the orientation of the HPL phase are confirmed, the internal structure of the film is not clearly seen from the two-dimensional TEM image. For the three-dimensional imaging of such a structure, TEMT is a powerful tool.[18] Figure 2a shows a part of a 3D image of the HPL structure obtained from TEMT. For visual clarity, only the PS domain is shown. The perforations in the layer structure are unambiguously observed. The positional repeating frequency is found in the image: the perforation at the edge of the first layer (shown by a vertical arrow) reappears at the same position in the fourth layer. This result indicates that the position of the perforations is repeated every three layers.

To make this clearer, three digitally sliced *x*−*z* planes corresponding to the first, third, and fourth layers are displayed in Figure 2b. As indicated by the dotted lines in the first layer, hexagonally arranged perforations in each layer were apparent. The relative positions of perforations in the three layers were examined in Figure 2c. The first and third layers exhibit a systematic shift of the perforation positions while the first and fourth layers showed a perfect match. Thus, the ABC type stacking, rather than the AB stacking, is evident in the HPL morphology. The ABC type stacking of the perforations is also confirmed by the GISAXS measurement as reported previously (the data are not shown).[17] The distance between the perforations measured by TEMT is ~29 nm, which is a little smaller than the value of 31.6 nm measured by GISAXS. Considering the slight skewness in the TEMT image and possible artifacts associated with the TEM measurement, they can be regarded as a reasonable match.

We also observed the coexistence of the two phases from the samples annealed at 120 °C for 30 h. Figure 3 is the cross-sectional TEM image of the structure showing the growth of the DG phase grain from the HPL structure. Repeated observations with multiple samples confirmed that the HPL to DG phase transition always starts from the substrate side. The mica surface

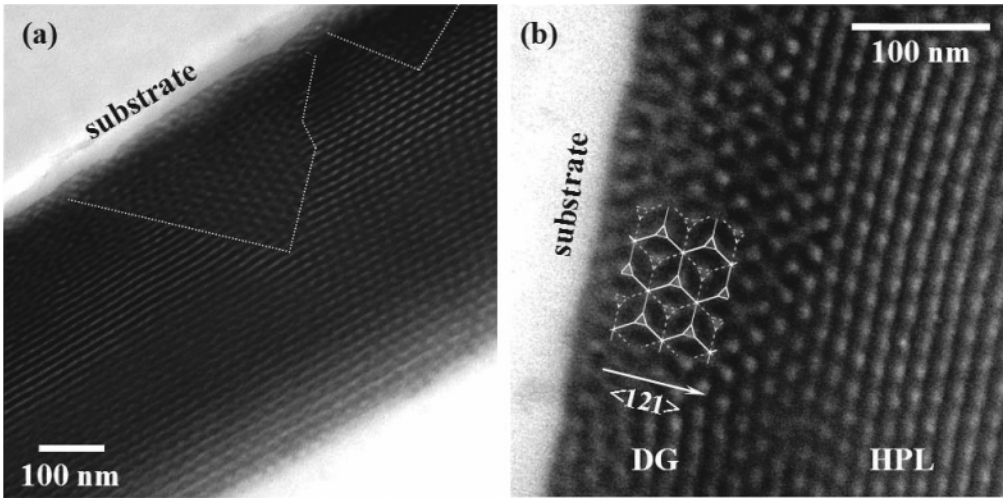

Figure 3. Cross-sectional TEM images of PS-*b*-PI thin film annealed 120 °C for 30 h, which show the coexistence of HPL and DG phases. (a) The HPL to DG phase transition always starts from the substrate side. Dotted lines are drawn for visual aid to identify the grain boundaries between the HPL and DG phases. The shape of the DG grain indicates that the nucleation is likely to take place at the substrate interface, and it grows outward. (b) The characteristic wagon wheel structure of {111} plane is clearly seen. The white lines depicting the DG {111} plane are drawn for visual aid.

must have induced the nucleation of the DG phase although the detailed mechanism remains to be elucidated. Figure 3b clearly shows that the characteristic wagon wheel structure of the {111} projection in the DG phase.

In summary, the phase transition of PS-*b*-PI thin film spin-coated on mica was investigated by cross-sectional TEM and TEMT. It was unambiguously confirmed that the HPL layers are oriented parallel to the substrate and the perforations have the ABC type stacking structure. The phase transition from HPL to DG phase in the PS-*b*-PI thin film on a mica substrate always starts from the substrate side, and the DG {121} plane is developed parallel to the substrate conforming to the epitaxial conversion between HPL layers and DG {121} plane.

Acknowledgment. T.C. and M.R. acknowledge the support from KOSEF (Center for Integrated Molecular Systems) and the BK21 program. The GISAXS measurements at PAL were supported by the Ministry of Science and Technology and POSCO. H.J. is grateful to NEDO for support through the Japanese National Project "Nano-Structured Polymer Project" by the Ministry of Economy, Trade and Industry and for support from the Ministry of Education, Science, Sports and Culture through Grant-in-Aid No. 1855019.

References and Notes

(1) Foerster, S.; Khandpur, A. K.; Zhao, J.; Bates, F. S.; Hamley, I. W.; Ryan, A. J.; Bras, W. *Macromolecules* **1994**, *27*, 6922−6935.
(2) Zhu, L.; Huang, P.; Chen, W. Y.; Weng, X.; Cheng, S. Z. D.; Ge, Q.; Quirk, R. P.; Senador, T.; Shaw, M. T.; Thomas, E. L.; Lotz, B.; Hsiao, B. S.; Yeh, F. J.; Liu, L. Z. *Macromolecules* **2003**, *36*, 3180−3188.
(3) Hamley, I. W.; Fairclough, J. P. A.; Ryan, A. J.; Mai, S. M.; Booth, C. *Phys. Chem. Chem. Phys.* **1999**, *1*, 2097−2101.
(4) Kimishima, K.; Koga, T.; Hashimoto, T. *Macromolecules* **2000**, *33*, 968−977.
(5) Koppi, K. A.; Tirrell, M.; Bates, F. S.; Almdal, K.; Mortensen, K. *J. Rheol. (N.Y., N.Y., U.S.)* **1994**, *38*, 999−1027.
(6) Krishnamoorti, R.; Silva, A. S.; Modi, M. A.; Hammouda, B. *Macromolecules* **2000**, *33*, 3803−3809.
(7) Lai, C. J.; Loo, Y. L.; Register, R. A.; Adamson, D. H. *Macromolecules* **2005**, *38*, 7098−7104.
(8) Lee, H. H.; Jeong, W. Y.; Kim, J. K.; Ihn, K. J.; Kornfield, J. A.; Wang, Z. G.; Qi, S. Y. *Macromolecules* **2002**, *35*, 785−794.
(9) Sakurai, S.; Kawada, H.; Hashimoto, T.; Fetters, L. J. *Macromolecules* **1993**, *26*, 5796−5802.
(10) Schulz, M. F.; Bates, F. S.; Almdal, K.; Mortensen, K. *Phys. Rev. Lett.* **1994**, *73*, 86−89.
(11) Zhao, J.; Majumdar, B.; Schulz, M. F.; Bates, F. S.; Almdal, K.; Mortensen, K.; Hajduk, D. A.; Gruner, S. M. *Macromolecules* **1996**, *29*, 1204−1215.
(12) Ryu, C. Y.; Lodge, T. P. *Macromolecules* **1999**, *32*, 7190−7201.
(13) Hajduk, D. A.; Gruner, S. M.; Rangarajan, P.; Register, R. A.; Fetters, L. J.; Honeker, C.; Albalak, R. J.; Thomas, E. L. *Macromolecules* **1994**, *27*, 490−501.
(14) Vigild, M. E.; Almdal, K.; Mortensen, K.; Hamley, I. W.; Fairclough, J. P. A.; Ryan, A. J. *Macromolecules* **1998**, *31*, 5702−5716.
(15) Hajduk, D. A.; Takenouchi, H.; Hillmyer, M. A.; Bates, F. S.; Vigild, M. E.; Almdal, K. *Macromolecules* **1997**, *30*, 3788−3795.
(16) Ahn, J. H.; Zin, W. C. *Macromol. Res.* **2003**, *11*, 152−156.
(17) Park, I.; Lee, B.; Ryu, J.; Im, K.; Yoon, J.; Ree, M.; Chang, T. *Macromolecules* **2005**, *38*, 10532−10536.
(18) Jinnai, H.; Nishikawa, Y.; Ikehara, T.; Nishi, T. *Adv. Polym. Sci.* **2004**, *170*, 115−167.
(19) Kwon, K.; Lee, W.; Cho, D.; Chang, T. *Korea Polym. J.* **1999**, *7*, 321−324.
(20) Lee, W.; Cho, D. Y.; Chang, T. Y.; Hanley, K. J.; Lodge, T. P. *Macromolecules* **2001**, *34*, 2353−2358.
(21) Lawrence, M. C. Least-squares method of alignment using markers. In *Electron Tomography: Three-Dimensional Imaging with the Transmission Electron Microscope*; Frank, J., Ed.; Plenum Press: New York, 1992.
(22) Crowther, R. A.; Derosier, D. J.; Klug, A. *Proc. R. Soc. London* **1970**, *317*, 319.
(23) Park, S.; Kwon, K.; Cho, D.; Lee, B.; Ree, M.; Chang, T. *Macromolecules* **2003**, *36*, 4662−4666.
(24) Lee, B.; Park, I.; Yoon, J.; Park, S.; Kim, J.; Kim, K. W.; Chang, T.; Ree, M. *Macromolecules* **2005**, *38*, 4311−4323.
(25) Koneripalli, N.; Levicky, R.; Bates, F. S.; Ankner, J.; Kaiser, H.; Satija, S. K. *Langmuir* **1996**, *12*, 6681−6690.
(26) Sohn, B. H.; Seo, B. W.; Yoo, S. I.; Zin, W. C. *Langmuir* **2002**, *18*, 10505−10508.
(27) Ludwigs, S.; Boker, A.; Voronov, A.; Rehse, N.; Magerle, R.; Krausch, G. *Nat. Mater.* **2003**, *2*, 744−747.
(28) Ludwigs, S.; Schmidt, K.; Stafford, C. M.; Amis, E. J.; Fasolka, M. J.; Karim, A.; Magerle, R.; Krausch, G. *Macromolecules* **2005**, *38*, 1850−1858.

MA062826C